Issue Contents

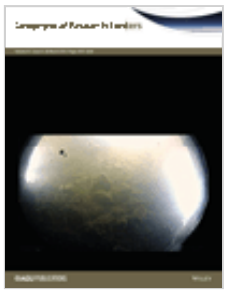

Volume 39, Issue 20

28 October 2012

Brief Detailed

Atmospheric Science

Detrainment in deep convection

S. J. Böing, A. P. Siebesma, J. D. Korpershoek, H. J. J. Jonker

First Published: 31 October 2012 Vol: 39, L20816 | DOI: 10.1029/2012GL053735

KEY POINTS

- Intensity of atmospheric deep convection governed by detrainment
- Detrainment closely coupled to free tropospheric stability and relative humidity
- Simple model captures sensitivity of detrainment to these variables

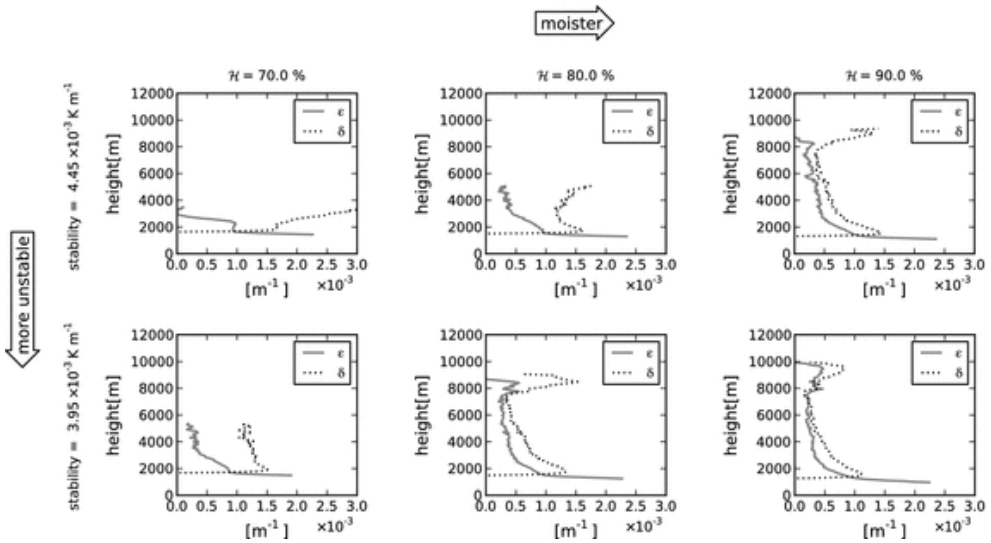

1 of 4

Traveling planetary-scale Rossby waves in the winter stratosphere: The role of tropospheric baroclinic instability

Daniela I. V. Domeisen, R. Alan Plumb

First Published: 31 October 2012 Vol: 39, L20817 | DOI: 10.1029/2012GL053684

KEY POINTS

- Stratospheric variability increases in an atmosphere without synoptic motions
- Synoptic waves weaken the generation of planetary waves
- Baroclinic instability of long waves causes stratospheric warmings

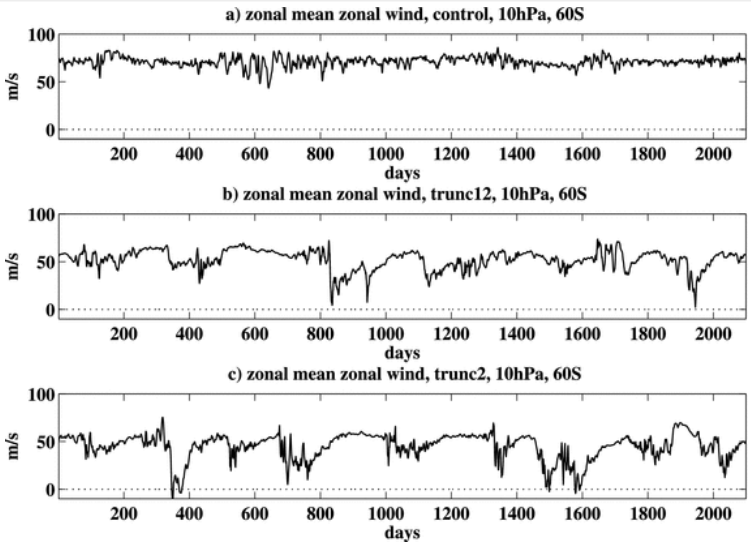

1 of 6

Lateral entrainment rate in shallow cumuli: Dependence on dry air sources and probability density functions

Chunsong Lu, Yangang Liu, Shengjie Niu, Andrew M. Vogelmann

First Published: 30 October 2012 Vol: 39, L20812 | DOI: 10.1029/2012GL053646

KEY POINTS

- Dependence of entrainment rate on dry air sources is studied for the first time
- Probability density functions of entrainment rate are studied for the first time
- Implications of the results for convection parameterizations are discussed

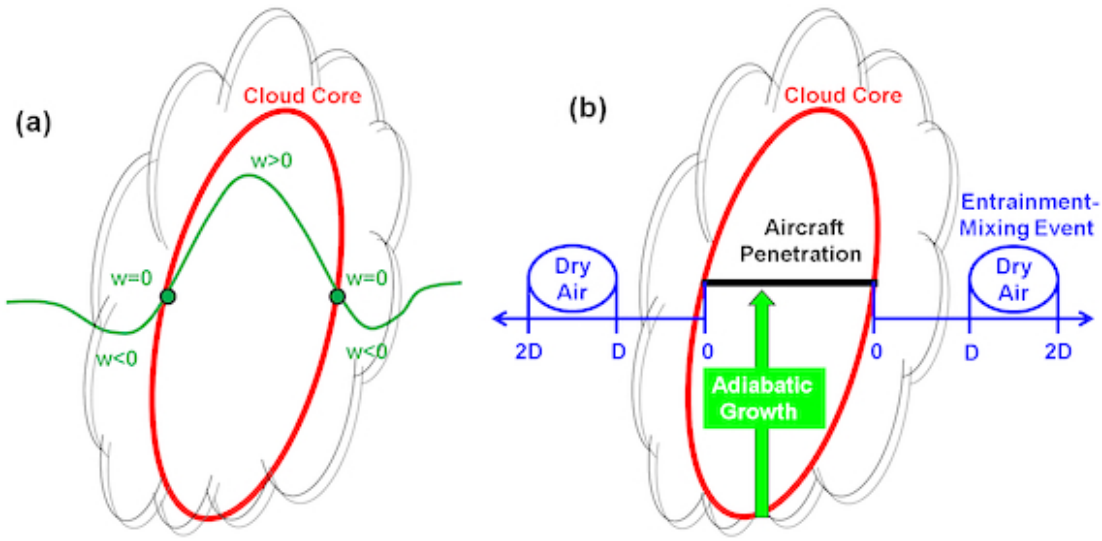

1 of 4

Identification of the biogenic compounds responsible for size-dependent nanoparticle growth

Paul M. Winkler, John Ortega, Thomas Karl, Luca Cappellin, Hans R. Friedli, Kelley Barsanti, Peter H. McMurry, James N. Smith

First Published: 30 October 2012 Vol: 39, L20815 | DOI: 10.1029/2012GL053253

KEY POINTS

- Chemical composition of biogenic nanoparticles is size-dependent
- Experimental data in good agreement with thermodynamic growth model
- High time resolution measurements needed to quantify nanoparticle growth

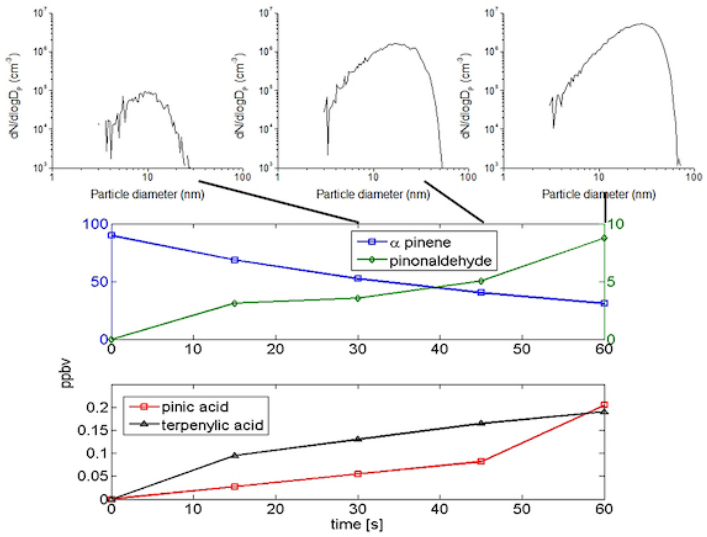

1 of 3

Modelling future changes to the stratospheric source gas injection of biogenic bromocarbons

R. Hossaini, M. P. Chipperfield, S. Dhomse, C. Ordóñez, A. Saiz-Lopez, N. L. Abraham, A. Archibald, P. Braesicke, P. Telford, N. Warwick, et al

First Published: 30 October 2012 Vol: 39, L20813 | DOI: 10.1029/2012GL053401

KEY POINTS

- Increased transport of VSLS to the stratosphere with climate change
- 2100 simulations show significant increase in Br from VSLS in lower stratosphere
- Significant differences in tropospheric oxidizing capacity between RCP 4.5 and 8.5

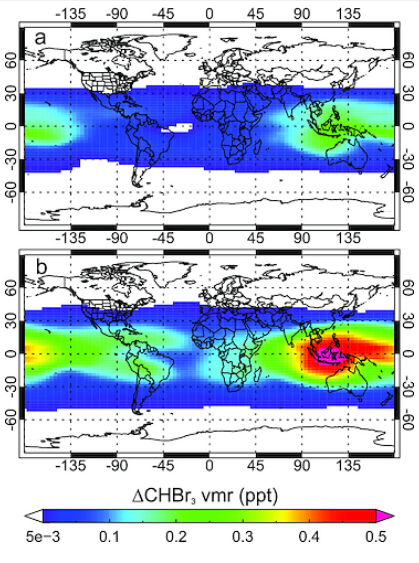

A conceptual model for self-sustained active-break Indian summer monsoon

Fei Liu, Bin Wang

First Published: 30 October 2012 Vol: 39, L20814 | DOI: 10.1029/2012GL053663

KEY POINTS

- Air-sea interaction is a key in sustaining Indian summer monsoon oscillation
- A precipitation dipole can develop more easily than a precipitation monopole
- Strong air-sea interaction will shorten the oscillation period

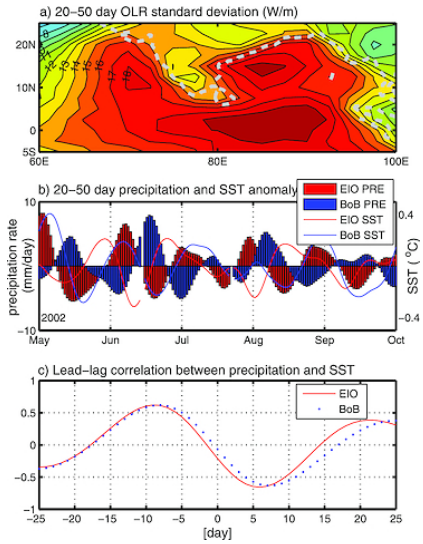

The influence of the SAL and lightning on tropospheric ozone variability over the Northern Tropical Atlantic: Results from Cape Verde during 2010

Gregory S. Jenkins, Miliaritiana L. Robjhon, Jonathan W. Smith, Jonathan Clark, Luis Mendes

First Published: 27 October 2012 Vol: 39, L20810 | DOI: 10.1029/2012GL053532

KEY POINTS

- The SAL leads to an increase in O3 values at its base
- There is evidence of reduced ozone above the SAL's base
- A large dust event on 8 July produced elevated ozone levels above the surface

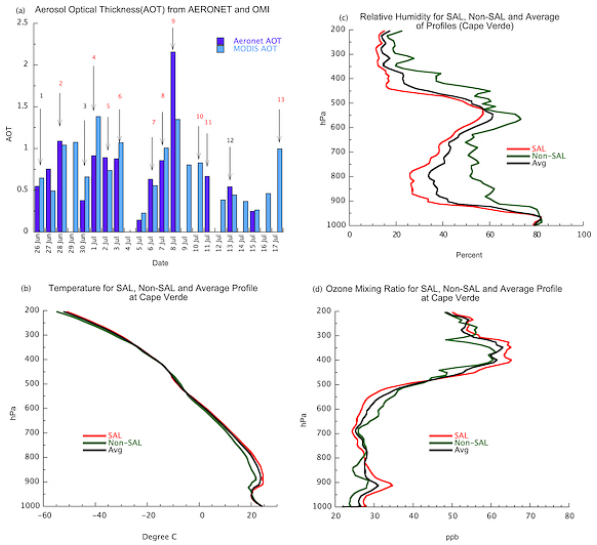

1 of 5

High supersaturation inside cirrus in well-developed tropical tropopause layer over Indonesia

Y. Inai, T. Shibata, M. Fujiwara, F. Hasebe, H. Vömel

First Published: 27 October 2012 Vol: 39, L20811 | DOI: 10.1029/2012GL053638

KEY POINTS

- Many cases of high supersaturations inside cirrus in the TTL were found
- The sensors for water vapor and cirrus were the most reliable instruments
- Dependence of supersaturation on phase of large-scale disturbance was suggested

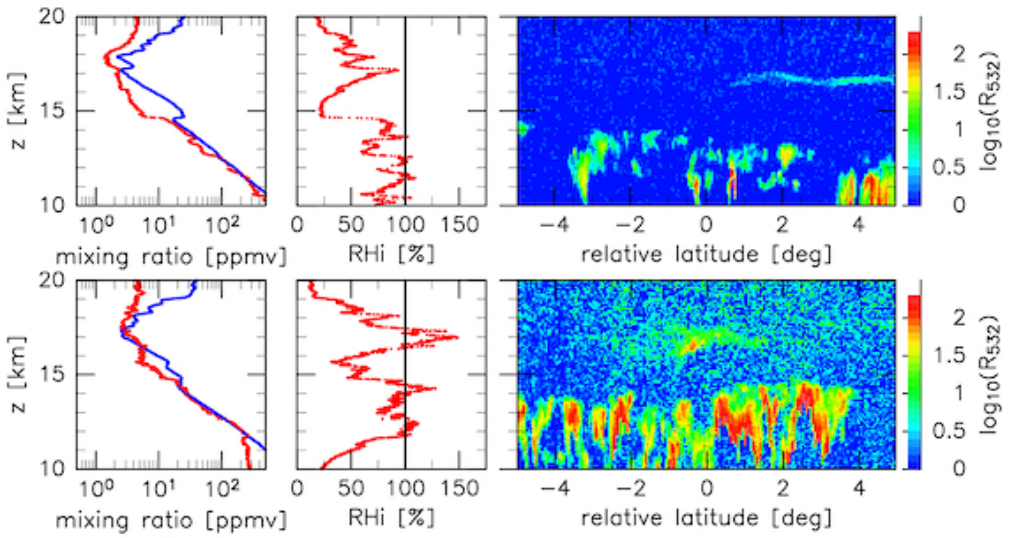

1 of 4

Relationship of environmental relative humidity with North Atlantic tropical cyclone intensity and intensification rate

Longtao Wu, Hui Su, Robert G. Fovell, Bin Wang, Janice T. Shen, Brian H. Kahn, Svetla M. Hristova-Veleva, Bjorn H. Lambrigtsen, Eric J. Fetzer, Jonathan H. Jiang

First Published: 24 October 2012 Vol: 39, L20809 | DOI: 10.1029/2012GL053546

KEY POINTS

- ERH above the boundary layer generally decreases with time
- ERH generally increase with increasing TC intensity and intensification rate
- At Q1, RI is associated with a sharp decrease of ERH in the UT

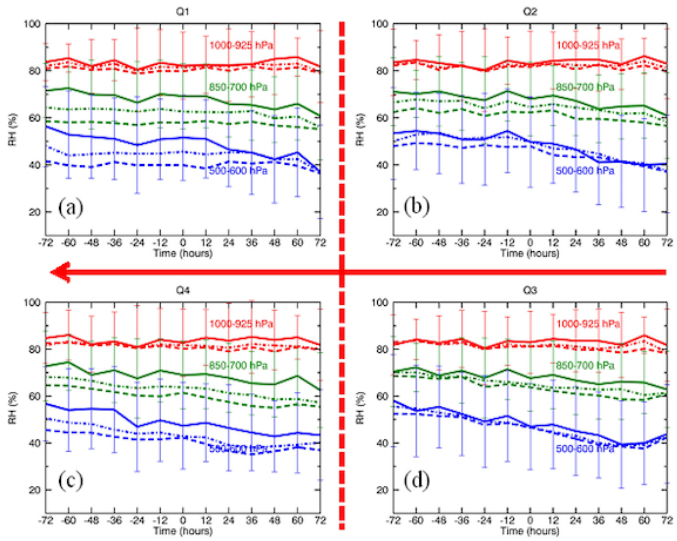

1 of 4

How may low-cloud radiative properties simulated in the current climate influence low-cloud feedbacks under global warming?

F. Brient, S. Bony

First Published: 23 October 2012 Vol: 39, L20807 | DOI: 10.1029/2012GL053265

KEY POINTS

- Correlation between low-cloud radiative effects in present and future climates
- Due to a positive radiative feedback between low clouds and relative humidity
- Observations help constrain the strength of climate change low-cloud feedbacks

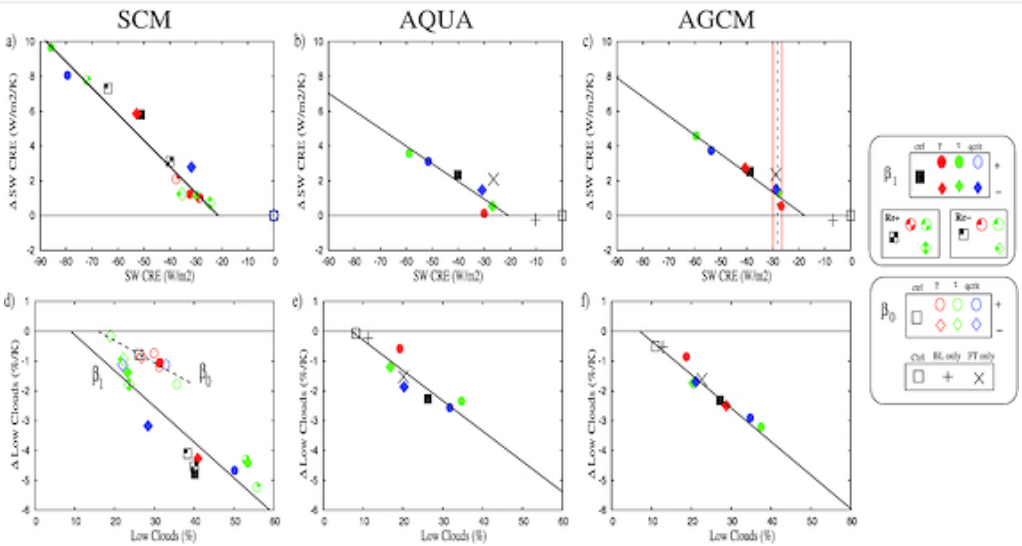

1 of 4

The MJO-Kelvin wave transition

A. H. Sobel, D. Kim
First Published: 23 October 2012 Vol: 39, L20808 | DOI: 10.1029/2012GL053380

KEY POINTS

- MJO events turn into Kelvin waves as they move east
- The transition often occurs in the Indian Ocean
- Apparent slow Kelvin waves in spectra may possibly be transitions

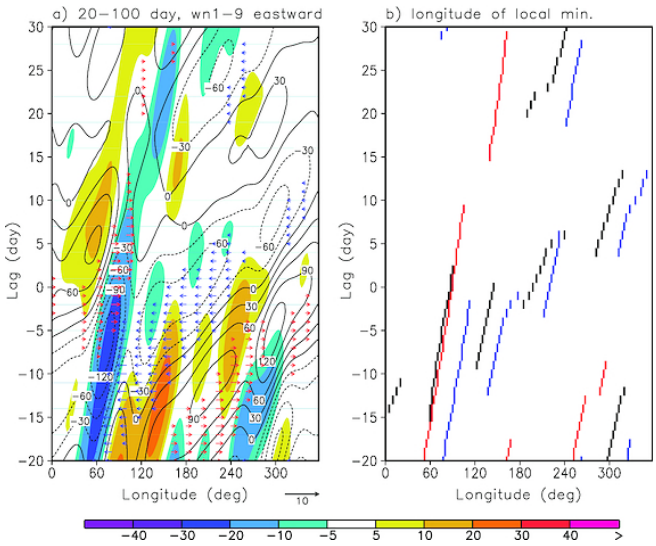

1 of 4

Aerosols in central California: Unexpectedly large contribution of coarse mode to aerosol radiative forcing

Evgueni Kassianov, Mikhail Pekour, James Barnard
First Published: 20 October 2012 Vol: 39, L20806 | DOI: 10.1029/2012GL053469

KEY POINTS

- Large contribution of coarse mode aerosol to total volume for clean area
- Important role of coarse mode aerosol in changing aerosol radiative forcing

Highlight

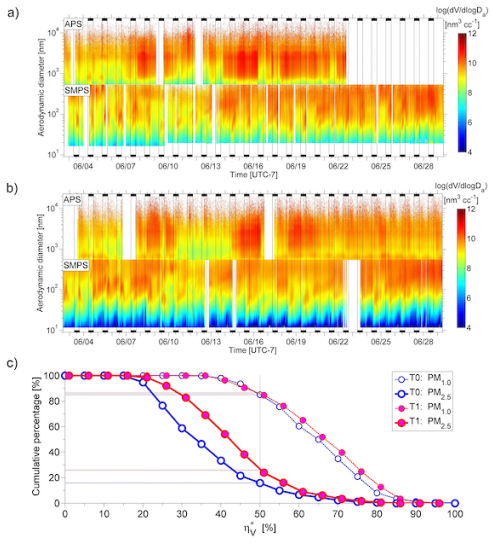

1 of 3

Ice cloud depolarization for nadir and off-nadir CALIPSO measurements

Kenneth Sassen, Vinay Kumar Kayetha, Jiang Zhu

First Published: 19 October 2012 Vol: 39, L20805 | DOI: 10.1029/2012GL053116

KEY POINTS

- Lidar depolarization in ice clouds varies significantly
- Lidar depolarization implies complicated simulations
- CALIPSO is a powerful tool for cloud research

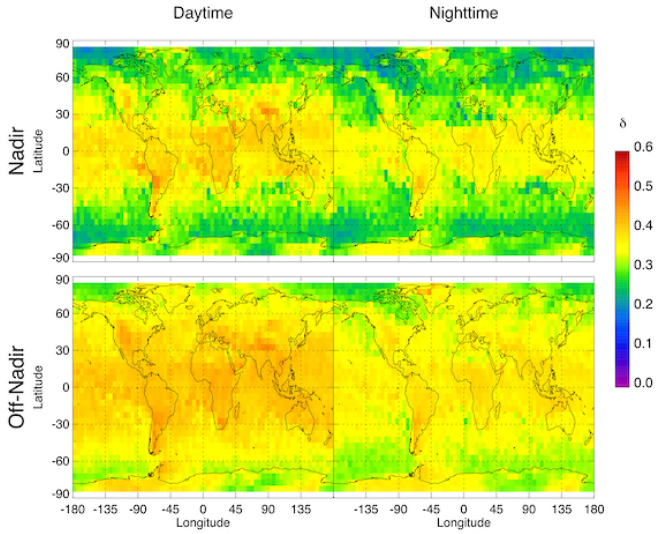

1 of 3

Ubiquitous low-level liquid-containing Arctic clouds: New observations and climate model constraints from CALIPSO-GOCCP

G. Cesana, J. E. Kay, H. Chepfer, J. M. English, G. de Boer

First Published: 19 October 2012 Vol: 39, L20804 | DOI: 10.1029/2012GL053385

KEY POINTS

- New CALIPSO-GOCCP observations show ubiquitous liquid-containing Arctic clouds
- Insufficient liquid-containing Arctic cloud leads to radiation biases in models
- Reproducing observed cloud phase is an important target for model improvement

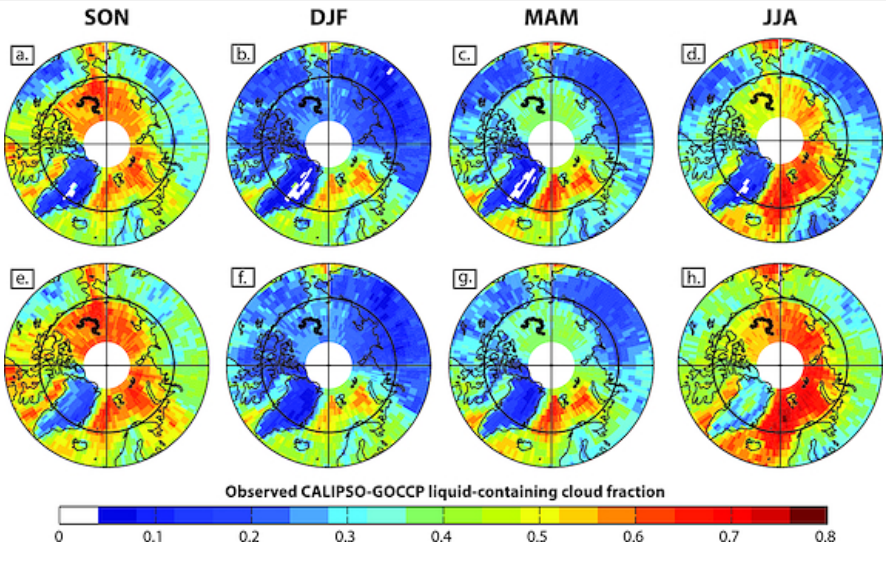

How well do climate models simulate cloud vertical structure? A comparison between CALIPSO-GOCCP satellite observations and CMIP5 models

G. Cesana, H. Chepfer

First Published: 19 October 2012 Vol: 39, L20803 | DOI: 10.1029/2012GL053153

KEY POINTS

- To evaluate the cloud vertical structure of models using CALIPSO satellite
- Five GCMs underestimate the total cloud cover at all latitudes except in Arctic
- Discrepancies are more pronounced in tropics and poles, and over continents

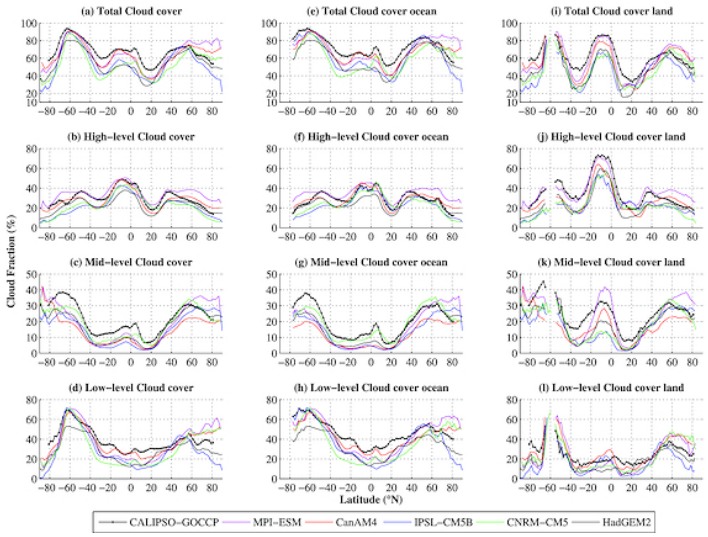

Fraction of natural area as main predictor of net CO_2 emissions from cities

Annika Nordbo, Leena Järvi, Sami Haapanala, Curtis R. Wood, Timo Vesala

First Published: 18 October 2012 Vol: 39, L20802 | DOI: 10.1029/2012GL053087

KEY POINTS

- Fraction of natural area can be used as a proxy for annual urban CO2 budgets
- The proxy's strength is corroborated using emission inventories from 56 cities
- The proxy is used for continental-scale mapping of urban CO2 emissions

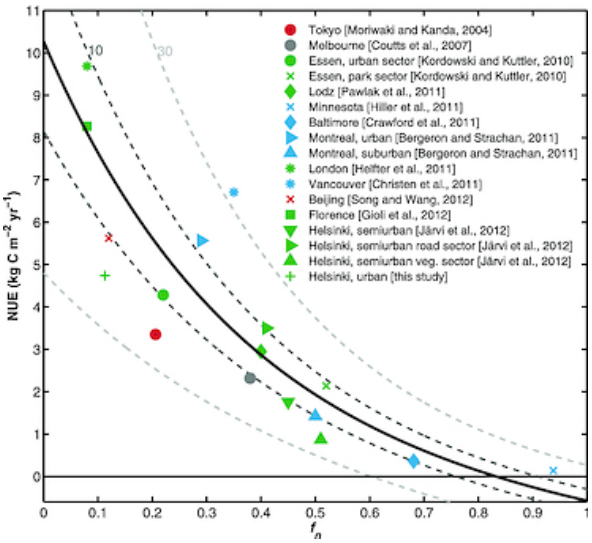

1 of 3

The vertical and spatial structure of ENSO in the upper troposphere and lower stratosphere from GPS radio occultation measurements

B. Scherllin-Pirscher, C. Deser, S.-P. Ho, C. Chou, W. Randel, Y.-H. Kuo

First Published: 17 October 2012 Vol: 39, L20801 | DOI: 10.1029/2012GL053071

KEY POINTS

- Utilize GPS radio occultation (RO) data to detect the 3-dim ENSO structure
- Coherent upper tropospheric and lower stratospheric ENSO signals
- Differences in zonal-mean and eddy ENSO components

Open Access

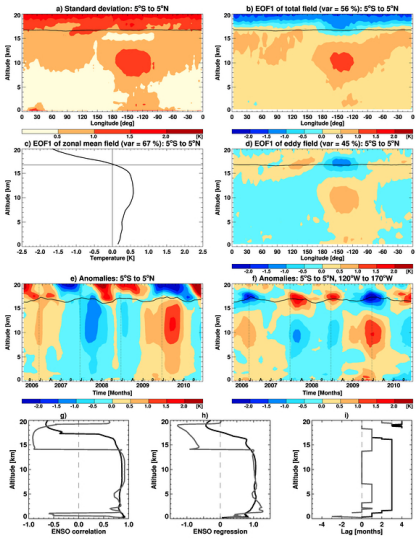

1 of 3

Climate

Correction to “Alternatives to stabilization scenarios”

D. J. Frame, D. A. Stone, P. A. Stott, M. R. Allen

First Published: 31 October 2012 Vol: 39, L20717 | DOI: 10.1029/2012GL053647

Relating the strength of the tropospheric biennial oscillation (TBO) to the phase of the Interdecadal Pacific Oscillation (IPO)

Gerald A. Meehl, Julie M. Arblaster

First Published: 30 October 2012 Vol: 39, L20716 | DOI: 10.1029/2012GL053386

KEY POINTS

- The phase of the IPO affects the amplitude of the TBO
- When the IPO is in a positive phase the TBO has low amplitude
- When the IPO is in a negative phase the TBO has high amplitude

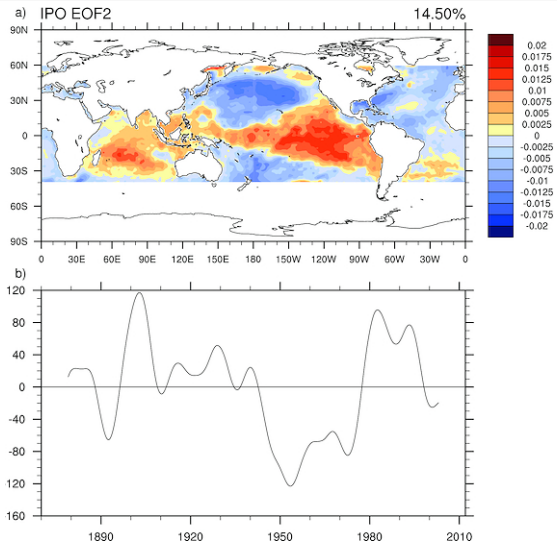

1 of 3

Increasing frequency, intensity and duration of observed global heatwaves and warm spells

S. E. Perkins, L. V. Alexander, J. R. Nairn

First Published: 27 October 2012 Vol: 39, L20714 | DOI: 10.1029/2012GL053361

KEY POINTS

- Global heatwaves have increased in frequency, intensity and duration
- Non-summer events are driving annual changes
- Nighttime heatwaves have increased faster than daytime and daily-average events

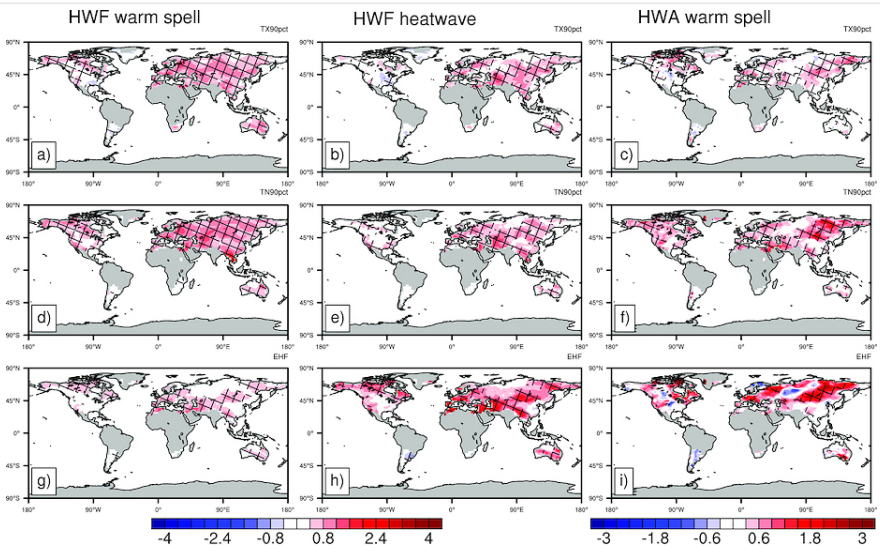

Spatial and glacial-interglacial variations in provenance of the Chinese Loess Plateau

Guoqiao Xiao, Keqing Zong, Gaojun Li, Zhaochu Hu, Guillaume Dupont-Nivet, Shuzhen Peng, Kexin Zhang

First Published: 27 October 2012 Vol: 39, L20715 | DOI: 10.1029/2012GL053304

KEY POINTS

- The provenance of Chinese loess is studied by detrital zircon ages
- The provenance of Chinese Loess Plateau is heterogeneous and spatially variable
- Glacial-interglacial provenance changes are coupled with the wind patterns

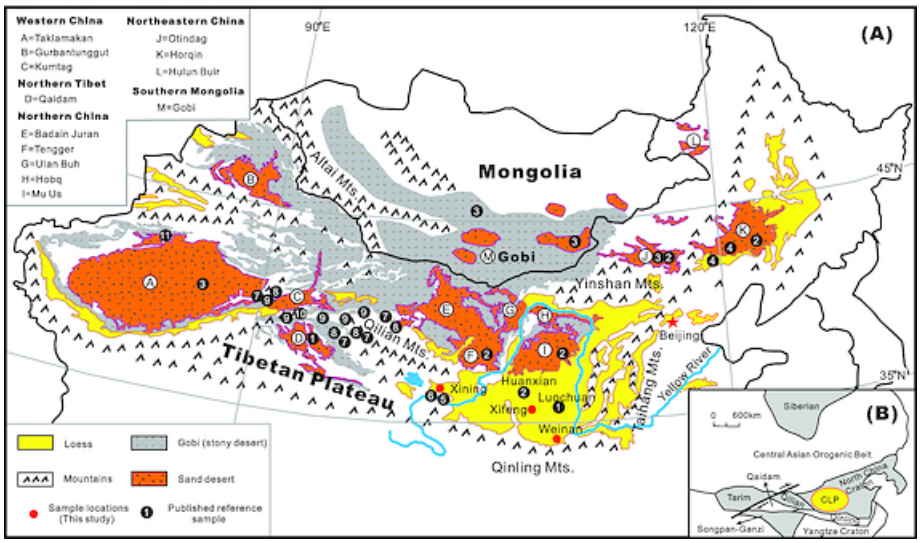

1 of 2

Evaluation of monsoon seasonality and the tropospheric biennial oscillation transitions in the CMIP models

Yue Li, Nicolas C. Jourdain, Andréa S. Taschetto, Caroline C. Ummenhofer, Karumuri Ashok, Alexander Sen Gupta

First Published: 26 October 2012 Vol: 39, L20713 | DOI: 10.1029/2012GL053322

KEY POINTS

- The Indian-Australian monsoon predictability to TBO is assessed in CMIP models
- CMIP5 models show improved simulation of Indian-Australian monsoon system
- Observations & CMIP show enhanced predictability of India-Australia transition

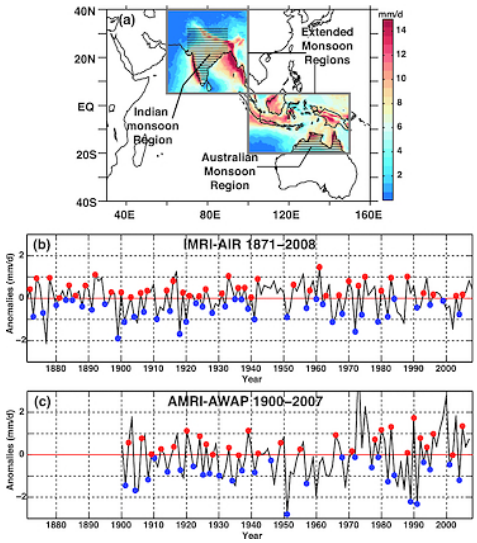

1 of 3

The decadal modulation of coupled bred vectors

Yoo-Geun Ham, Michele M. Rienecker, Siegfried Schubert, Jelena Marshak, Sang-Wook Yeh, Shu-Chih Yang

First Published: 25 October 2012 Vol: 39, L20712 | DOI: 10.1029/2012GL053719

KEY POINTS

- The nature of a decadal modulation in the coupled bred vectors (BVs) is examined
- The decadal location shift of BV is consistent with El Nino action center shift
- This shift is due to the strengthening of the mean zonal temperature gradient

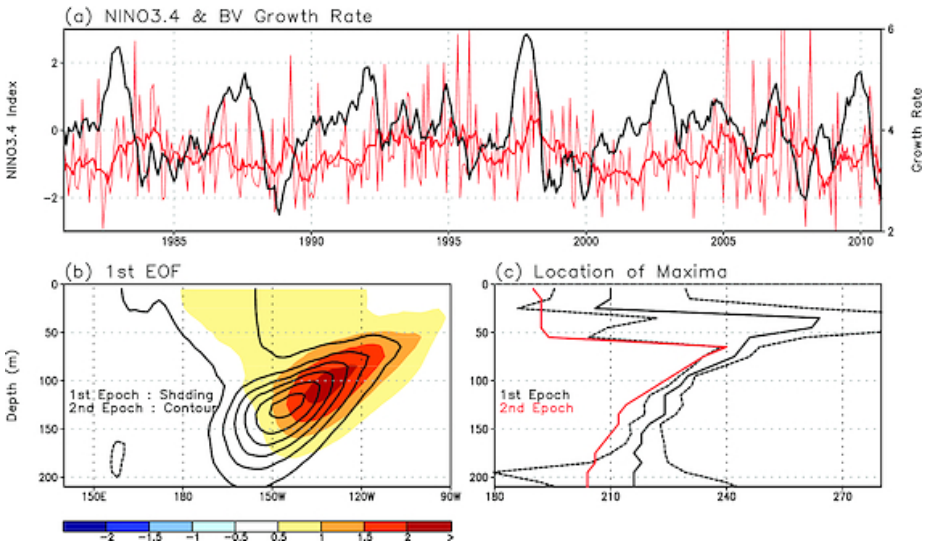

1 of 4

Clouds and Snowball Earth deglaciation

Dorian S. Abbot, Aiko Voigt, Mark Branson, Raymond T. Pierrehumbert, David Pollard, Guillaume Le Hir, Daniel D. B. Koll

First Published: 25 October 2012 Vol: 39, L20711 | DOI: 10.1029/2012GL052861

KEY POINTS

- We run a suite of GCMs with Snowball Earth boundary conditions

- We find that clouds can reduce the CO2 needed to deglaciate by 10-100
- Snowball deglaciation no longer seems a serious problem for the hypothesis

Highlight

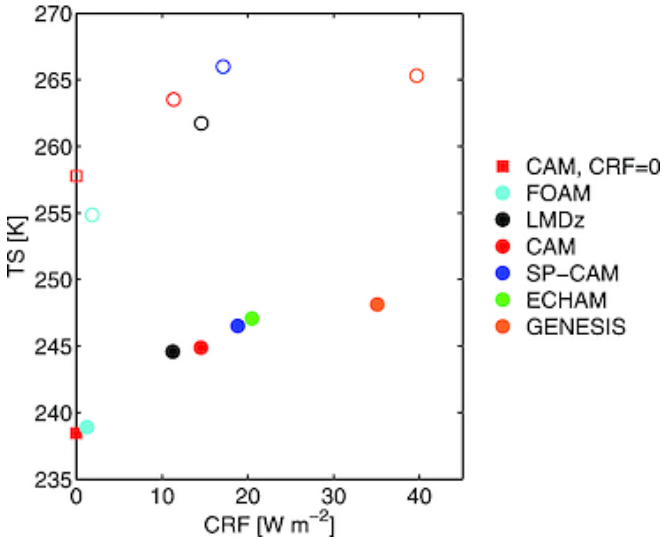

1 of 3

Can aerosol loading explain the solar dimming over the Tibetan Plateau?

Kun Yang, Baohong Ding, Jun Qin, Wenjun Tang, Ning Lu, Changgui Lin

First Published: 24 October 2012 Vol: 39, L20710 | DOI: 10.1029/2012GL053733

KEY POINTS

- Solar dimming and total cloud cover decreasing co-existed
- Aerosol impact on solar dimming was not significant over TP
- Deep cloud cover and water vapor content increased

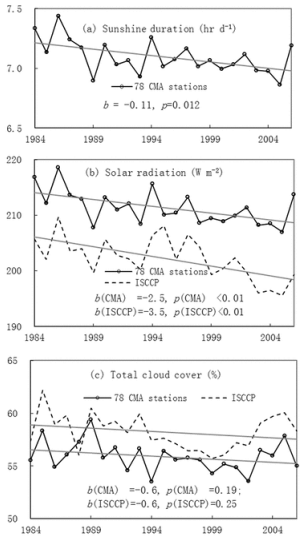

1 of 5

Stability of the Atlantic meridional overturning circulation: A model intercomparison

Andrew J. Weaver, Jan Sedláček, Michael Eby, Kaitlin Alexander, Elisabeth Crespin, Thierry Fichefet,

Gwenaëlle Philippon-Berthier, Fortunat Joos, Michio Kawamiya, Katsumi Matsumoto, et al

First Published: 24 October 2012 Vol: 39, L20709 | DOI: 10.1029/2012GL053763

KEY POINTS

- All climate models project very similar behavior during the 21st century
- No model exhibits an abrupt change of the MOC
- More than 1/2 of the models are in the bistable regime ==> not overly stable

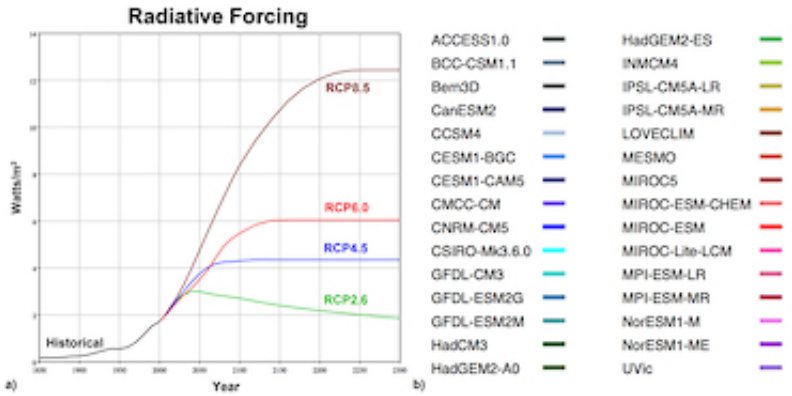

1 of 4

Evidence for external forcing on 20th-century climate from combined ocean-atmosphere warming patterns

Jan Sedláček, Reto Knutti

First Published: 23 October 2012 Vol: 39, L20708 | DOI: 10.1029/2012GL053262

KEY POINTS

- Ocean warming of the last century cannot be explained by natural variability
- The warming signal is visible throughout the whole ocean
- Forced patterns are smooth and patterns of natural variability are heterogeneous

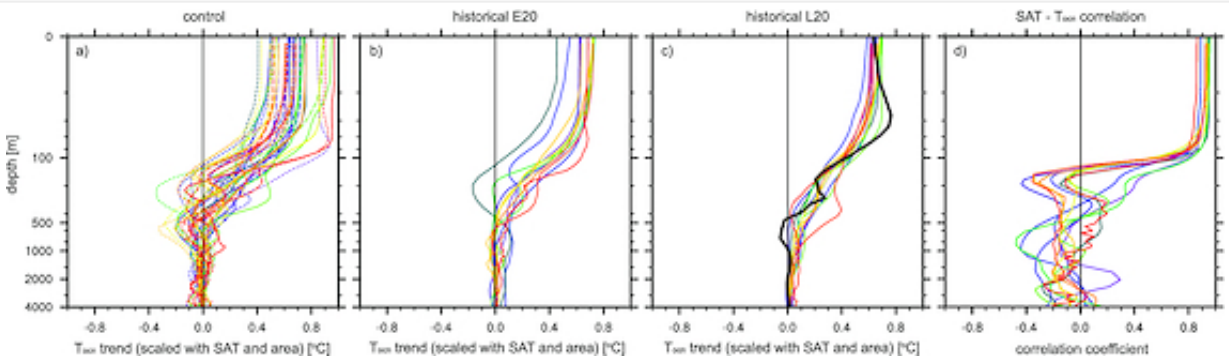

1 of 3

Trends in the global tropopause thickness revealed by radiosondes

Sha Feng, Yunfei Fu, Qingnong Xiao

First Published: 20 October 2012 Vol: 39, L20706 | DOI: 10.1029/2012GL053460

KEY POINTS

- Tropopause layer has been thickening in recent decades for the entire globe
- Remarkable rising trends are observed in the top of TL
- The entire TL may be raised for positive trends in both the bottom and top of it

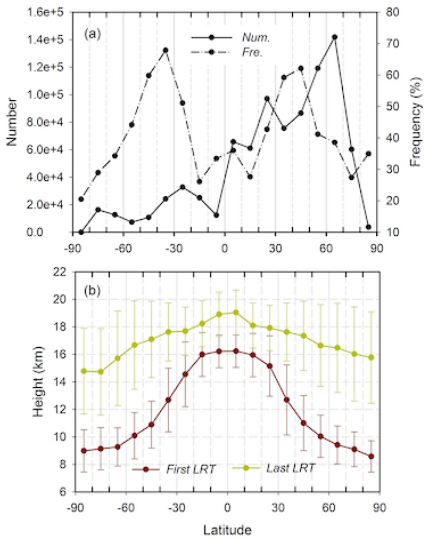

1 of 4

Arctic sea ice reduction and European cold winters in CMIP5 climate change experiments

Shuting Yang, Jens H. Christensen

First Published: 20 October 2012 Vol: 39, L20707 | DOI: 10.1029/2012GL053338

KEY POINTS

- Probability of European cold winters in the future
- Linkage between European cold winters and the Barents-Kara Sea ice reduction
- CMIP5 analysis

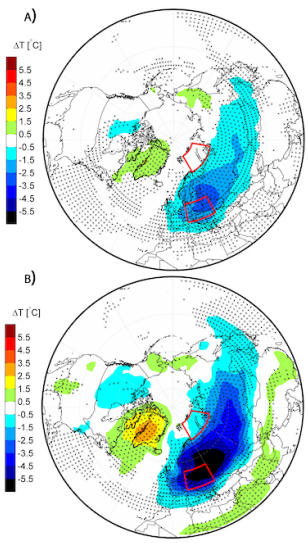

1 of 4

Antarctic climate response to stratospheric ozone depletion in a fine resolution ocean climate model

C. M. Bitz, L. M. Polvani
First Published: 19 October 2012 Vol: 39, L20705 | DOI: 10.1029/2012GL053393

KEY POINTS

- It is unlikely that ozone depletion caused recent Antarctic sea ice expansion
- The sea ice response is similar with resolved and parameterized eddies
- The ocean warming is more moderate when eddies are resolved

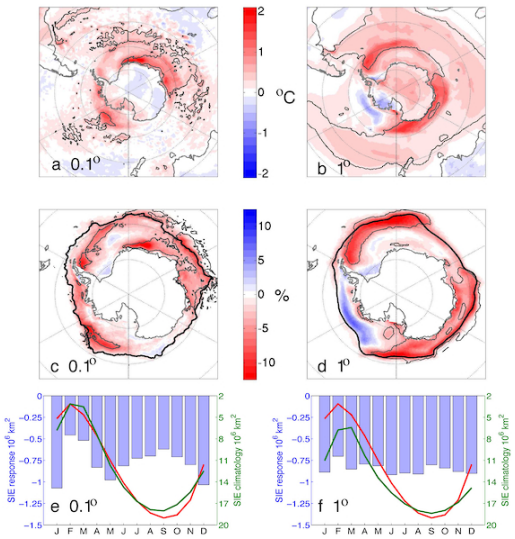

1 of 4

Impact of solar-induced stratospheric ozone decline on Southern Hemisphere westerlies during the Late Maunder Minimum

V. Varma, M. Prange, T. Spangehl, F. Lamy, U. Cubasch, M. Schulz
First Published: 19 October 2012 Vol: 39, L20704 | DOI: 10.1029/2012GL053403

KEY POINTS

- Southern westerlies and stratospheric ozone during Late Maunder Minimum
- Application of coupled climate modeling
- Support for model evidence from reconstructed data

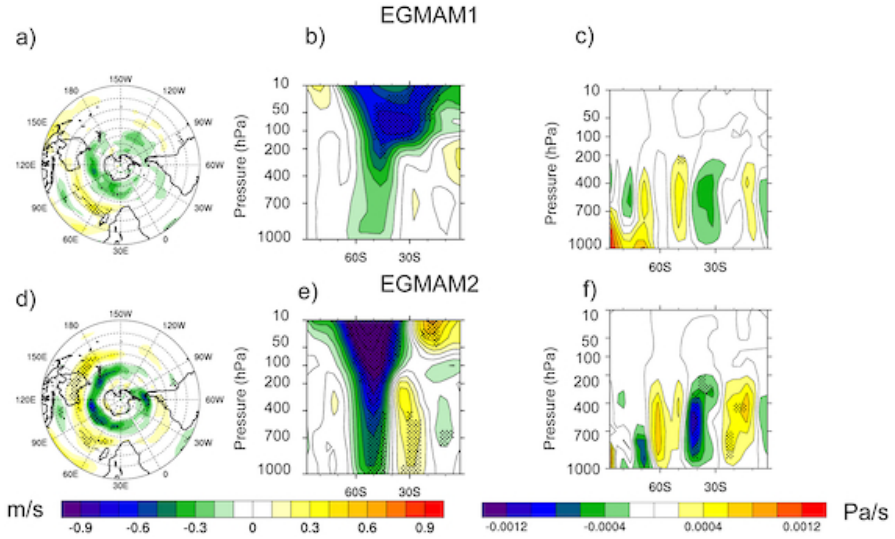

1 of 4

Uncertainty in the ENSO amplitude change from the past to the future

Masahiro Watanabe, Jong-Seong Kug, Fei-Fei Jin, Mat Collins, Masamichi Ohba, Andrew T. Wittenberg

First Published: 17 October 2012 Vol: 39, L20703 | DOI: 10.1029/2012GL053305

KEY POINTS

- We constructed perturbed physics ensembles (PPEs) to examine ENSO changes
- Nino3 mean precip gives a good metric of ENSO amplitude in PPEs and also in MME
- Detectable ENSO amplification from the past to present, explained by #2

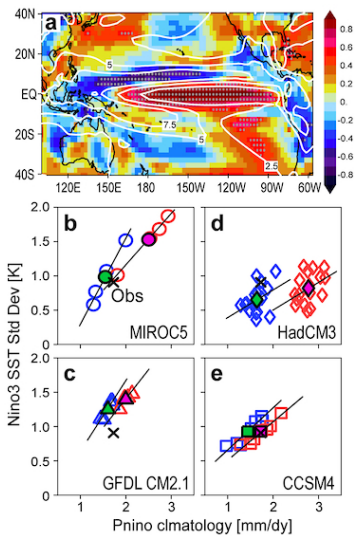

1 of 4

The impact of the El Niño-Southern Oscillation on maximum temperature extremes

Julie M. Arblaster, Lisa V. Alexander

First Published: 16 October 2012 Vol: 39, L20702 | DOI: 10.1029/2012GL053409

KEY POINTS

- Marked contrasts in observed maximum temperature extremes during ENSO phases
- Two coupled models show ENSO fidelity crucial for impact on temperature extremes

- Similar relationships found in a simulation of future climate change

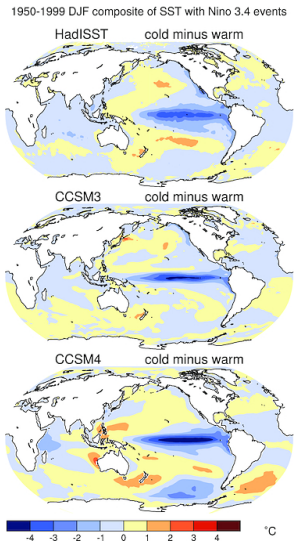

1 of 3

Mitigation of 21st century Antarctic sea ice loss by stratospheric ozone recovery

Karen L. Smith, Lorenzo M. Polvani, Daniel R. Marsh

First Published: 16 October 2012 Vol: 39, L20701 | DOI: 10.1029/2012GL053325

KEY POINTS

- Stratospheric ozone recovery will mitigate Antarctic projected sea ice loss
- Ocean temperatures affect Antarctic sea ice on longer time scales, not the SAM
- Regulation of CFCs has climate impacts beyond the reduction of UV radiation

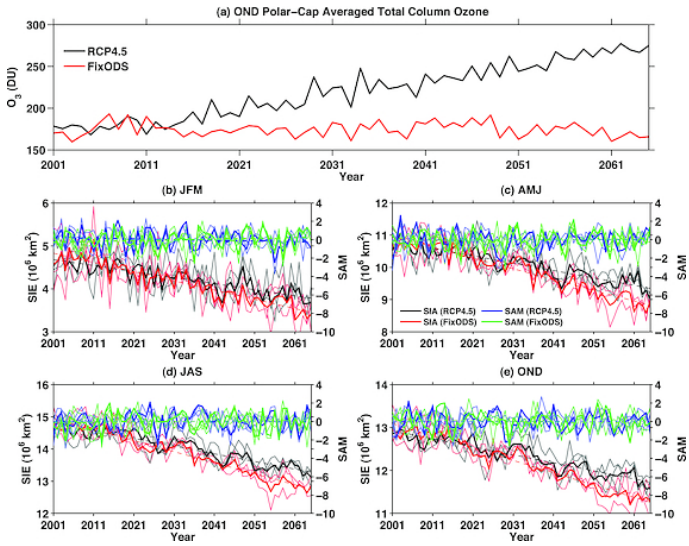

1 of 4

Hydrology and Land Surface Studies

Linking fluvial bed sediment transport across scales

Yong Zhang, Mark M. Meerschaert, Aaron I. Packman

First Published: 23 October 2012 Vol: 39, L20404 | DOI: 10.1029/2012GL053476

KEY POINTS

- Quantify sediment transport across scales using a unified stochastic model
- Explain the variance scaling of bed-load transport
- Test the random-walk model using well-known experiments

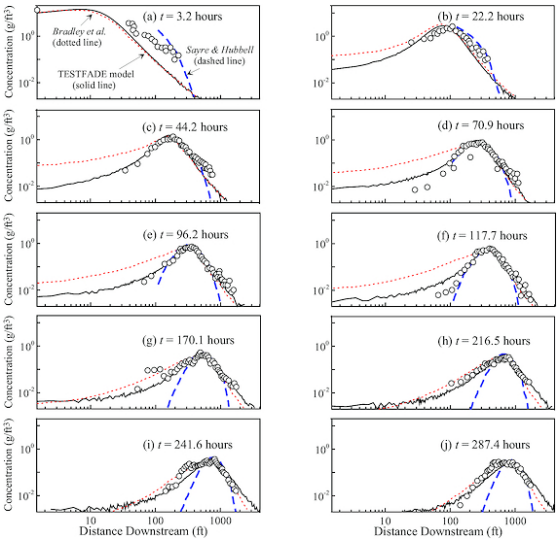

1 of 2

Mixing, entropy and reactive solute transport

Gabriele Chiogna, David L. Hochstetler, Alberto Bellin, Peter K. Kitanidis, Massimo Rolle
First Published: 23 October 2012 Vol: 39, L20405 | DOI: 10.1029/2012GL053295

KEY POINTS

- Application of information entropy to reactive solute transport problems
- Metrics for mixing: flux-related dilution index and its rate of change
- Quantification of complex interplay between dilution and reaction processes

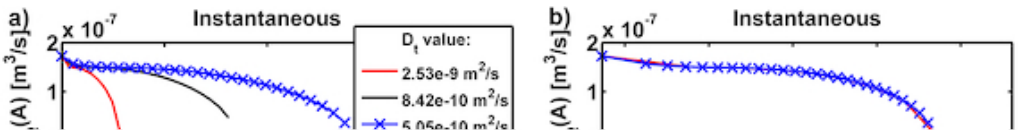

1 of 3

Interception of the Fukushima reactor accident-derived ^{137}Cs, ^{134}Cs and ^{131}I by coniferous forest canopies

Hiroaki Kato, Yuichi Onda, Takashi Gomi

First Published: 19 October 2012 Vol: 39, L20403 | DOI: 10.1029/2012GL052928

KEY POINTS

- Initial behavior of deposited radionuclides is examined in a forest environment
- Contrastive canopy interception was found between radiocesium and I-131
- Marked penetration of I-131 through forest canopy was observed

Highlight

1 of 3

Has the Three-Gorges Dam made the Poyang Lake wetlands wetter and drier?

Q. Zhang, L. Li, Y.-G. Wang, A. D. Werner, P. Xin, T. Jiang, D. A. Barry

First Published: 18 October 2012 Vol: 39, L20402 | DOI: 10.1029/2012GL053431

KEY POINTS

- The 3GD induces major changes in the downstream river discharge near the dam
- The 3GD causes considerable effects on the Poyang Lake water level
- The lake behavior is controlled by local factors modulated by the dam

Two dimensional bias correction of temperature and precipitation copulas in climate models

C. Piani, J. O. Haerter
First Published: 16 October 2012 Vol: 39, L20401 | DOI: 10.1029/2012GL053839

KEY POINTS

- A full 2D bias correction was developed
- Tested using temperature and precipitation copulas
- Results are positive for all observation stations used

Oceans

Autonomous underwater gliders monitoring variability at “choke points” in our ocean system: A case study in the Western Mediterranean Sea

Emma E. Heslop, Simón Ruiz, John Allen, José Luís López-Jurado, Lionel Renault, Joaquín Tintoré
First Published: 31 October 2012 Vol: 39, L20604 | DOI: 10.1029/2012GL053717

KEY POINTS

- New glider monitoring reveals hidden high variability in inter basin exchanges
- Glider flight parameters are ideal for monitoring critical ocean choke points

1 of 3

Haline hurricane wake in the Amazon/Orinoco plume: AQUARIUS/SACD and SMOS observations

Semyon A. Grodsky, Nicolas Reul, Gary Lagerloef, Gilles Reverdin, James A. Carton, Bertrand Chapron, Yves Quilfen, Vladimir N. Kudryavtsev, Hsun-Ying Kao

First Published: 18 October 2012 Vol: 39, L20603 | DOI: 10.1029/2012GL053335

KEY POINTS

- Hurricane passage produces a high salinity wake in areas of barrier layer
- Destruction of this barrier layer decreases SST cooling
- Decreased SST cooling results in less negative feedback on a hurricane

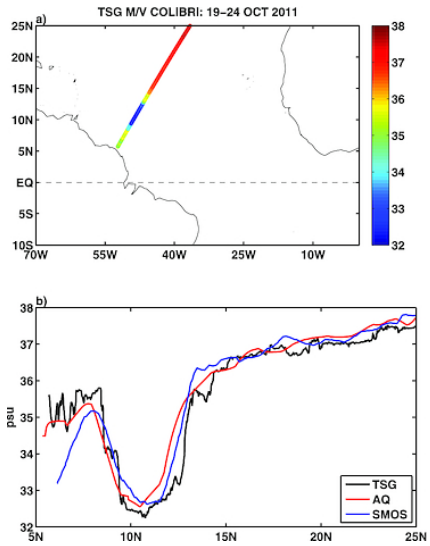

1 of 6

Deep mesoscale eddies in the Canada Basin, Arctic Ocean

J. R. Carpenter, M.-L. Timmermans

First Published: 17 October 2012 Vol: 39, L20602 | DOI: 10.1029/2012GL053025

KEY POINTS

- An active deep eddy field is observed in the Arctic Ocean
- The eddy field is spatially localized and derives from the same source
- We identify an outflow mechanism for eddy formation and vertical structure

1 of 4

The reduction of storm surge by vegetation canopies: Three-dimensional simulations

Y. Peter Sheng, Andrew Lapetina, Gangfeng Ma
First Published: 16 October 2012 Vol: 39, L20601 | DOI: 10.1029/2012GL053577

KEY POINTS
- Vegetation reduces coastal surge flooding 5-40%
- Vegetation dissipation increases with hurricane intensity and forward speed
- Vegetation dissipation increases with canopy height, density, and width

1 of 5

Planets

First observation of the Venus UV dayglow at limb from SPICAV/VEX

Jean-Yves Chaufray, Jean-Loup Bertaux, Francois Leblanc
First Published: 31 October 2012 Vol: 39, L20201 | DOI: 10.1029/2012GL053626

KEY POINTS
- First observations of the brightest UV airglow emissions on Venus
- First vertical profiles of a dayglow emission associated to CO2
- Comparison between Mars and Venus UV dayglow

1 of 3

Solid Earth

Electrical conductivity of magnetite-bearing serpentinite during shear deformation

Seiya Kawano, Takashi Yoshino, Ikuo Katayama
First Published: 30 October 2012 Vol: 39, L20313 | DOI: 10.1029/2012GL053652

KEY POINTS

- Percolation threshold for magnetite in serpentinite is 25 vol.%
- Shear deformation does not induce establishment of magnetite connectivity
- Magnetite-bearing serpentinite is not a cause of the conductivity anomaly

1 of 3

Complex characteristics of slow slip events in subduction zones reproduced in multi-cycle simulations

Harmony V. Colella, James H. Dieterich, Keith Richards-Dinger, Allan M. Rubin
First Published: 27 October 2012 Vol: 39, L20312 | DOI: 10.1029/2012GL053276

KEY POINTS

- Simulations of SSEs reproduce complex tremor migration patterns remarkably well
- Analytical solutions support results from our numerical modeling method
- Results suggest rapid back propagation is a consequence of frictional healing

1 of 4

Singing-sand avalanches without dunes

S. Dagois-Bohy, S. Courrech du Pont, S. Douady
First Published: 26 October 2012 Vol: 39, L20310 | DOI: 10.1029/2012GL052540

KEY POINTS

- Singing sand can emit sound during avalanches like in the field without a dune
- By sieving the grains, one can separate the frequencies emitted
- Frequency peaks correspond to the peaks in the grain size distribution

1 of 5

How do volcanic rift zones relate to flank instability? Evidence from collapsing rifts at Etna

Joel Ruch, Susi Pepe, Francesco Casu, Valerio Acocella, Marco Neri, Giuseppe Solaro, Eugenio Sansosti
First Published: 24 October 2012 Vol: 39, L20311 | DOI: 10.1029/2012GL053683

KEY POINTS

- First evidence of steady-state volcano rift instability at basaltic volcanoes
- New insights between magmatism and flank instability relationships at volcanoes

- Increase InSAR coherence on the summit of seasonally snow-capped volcanoes

1 of 3

P-V-T equation of state for *ε*-iron up to 80 GPa and 1900 K using the Kawai-type high pressure apparatus equipped with sintered diamond anvils

Daisuke Yamazaki, Eiji Ito, Takashi Yoshino, Akira Yoneda, Xinzhuan Guo, Baohua Zhang, Wei Sun, Akira Shimojuku, Noriyoshi Tsujino, Takehiro Kunimoto, et al

First Published: 23 October 2012 Vol: 39, L20308 | DOI: 10.1029/2012GL053540

KEY POINTS

- Precise determination of volume at high temperature under pressure
- Newly developed pressure generation technique enable us to do this research
- Density deficit of inner core of ~3% is largely smaller than that of outer core

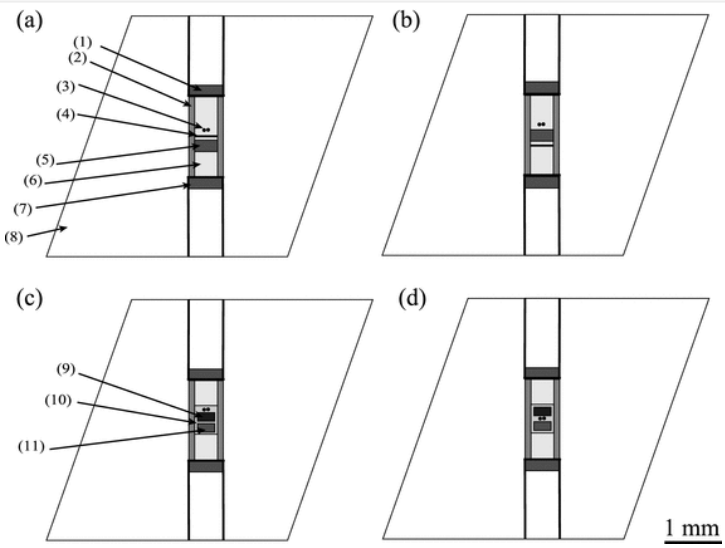

1 of 4

The great escape: An intra-Messinian gas system in the eastern Mediterranean

Michael Lazar, Uri Schattner, Moshe Reshef

First Published: 23 October 2012 Vol: 39, L20309 | DOI: 10.1029/2012GL053484

KEY POINTS

- Unique exposure of deep basin sea floor destabilized sub-sea floor gas systems
- Lowering sea levels allow gas to escape to water column and atmosphere
- Tectonic driven Mediterranean desiccation induced Mid-Messinian climatic shift

Out-of-sequence thrusting in experimental Coulomb wedges: Implications for the structural development of mega-splay faults and forearc basins

Saad S. B. Haq

First Published: 20 October 2012 Vol: 39, L20306 | DOI: 10.1029/2012GL053176

KEY POINTS

- Small variations in strength cause reorganization of deformation in a wedge
- Out-of-sequence faulting is inevitable in frontally accreting wedges
- Out-of-sequence backthrusting may be as common as forethrusting

Long period seismic source characterization at Popocatépetl volcano, Mexico

Alejandra Arciniega-Ceballos, Phillip Dawson, Bernard A. Chouet
First Published: 20 October 2012 Vol: 39, L20307 | DOI: 10.1029/2012GL053494

KEY POINTS

- Source properties quantification of long-period signals at Popocatepetl volcano
- Imagining seismic source mechanism associated with LP and VLP seismicity
- LP and VLP seismicity obey interaction of magmatic and hydrothermal processes

Open Access

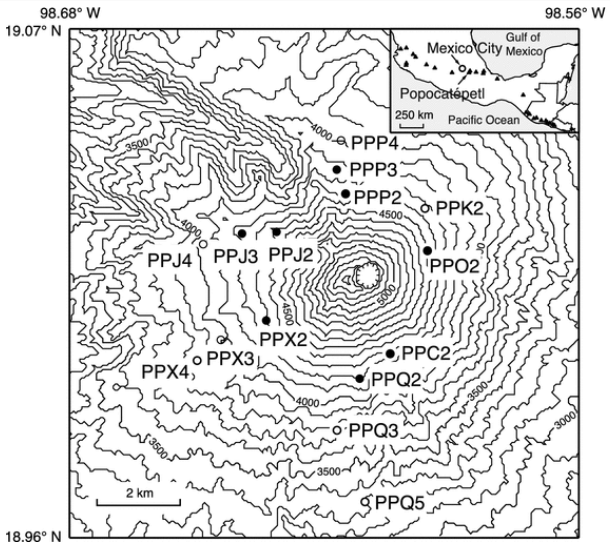

1 of 3

Decade-scale decrease in *b* value prior to the *M*9-class 2011 Tohoku and 2004 Sumatra quakes

K. Z. Nanjo, N. Hirata, K. Obara, K. Kasahara
First Published: 18 October 2012 Vol: 39, L20304 | DOI: 10.1029/2012GL052997

KEY POINTS

- Decrease in b value is a precursor to the M9-class Tohoku and Sumatra quakes
- The b value is an important indicator of an impending great earthquake
- The first report on M9-class quakes to confirm a change in b value

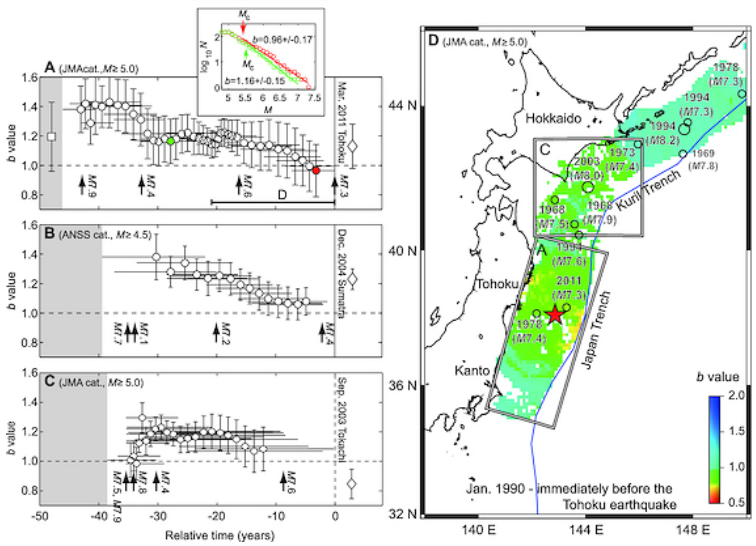

1 of 2

New detection of tremor triggered in Hokkaido, northern Japan by the 2004 Sumatra–Andaman earthquake

Kazushige Obara

First Published: 18 October 2012 Vol: 39, L20305 | DOI: 10.1029/2012GL053339

KEY POINTS

- Triggered tremor was detected where tectonic tremor has not been detected
- One tremor activity is close to source of volcanic low-frequency earthquake
- Another tremor activity correlates with compressional strain by surface wave

1 of 4

Challenging the rate-state asperity model: Afterslip following the 2011 M9 Tohoku-oki, Japan, earthquake

Kaj M. Johnson, Jun'ichi Fukuda, Paul Segall

First Published: 17 October 2012 Vol: 39, L20302 | DOI: 10.1029/2012GL052901

KEY POINTS

- Postseismic deformation is inconsistent with the rate-state asperity model
- Afterslip occurred on asperities or stress accumulated between asperities
- The simple asperity model for subduction zone coupling needs modification

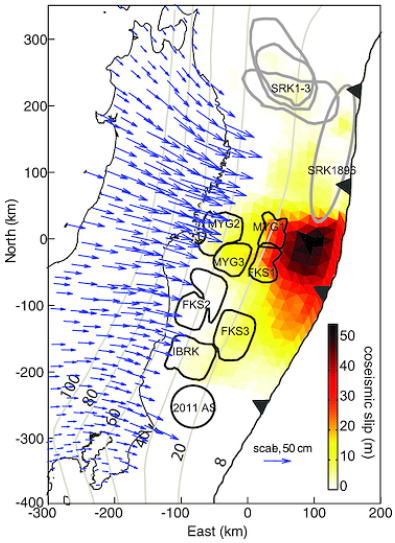

1 of 4

Seismic-afterslip characterization of the 2010 M_W 8.8 Maule, Chile, earthquake based on moment tensor inversion

Hans Agurto, Andreas Rietbrock, Isabelle Ryder, Matthew Miller

First Published: 17 October 2012 Vol: 39, L20303 | DOI: 10.1029/2012GL053434

KEY POINTS

- Seismic afterslip occurs mostly offshore in between patches of co-seismic slip
- Major aftershocks occur on the megathrust, in areas of medium coseismic slip
- High co-seismic slip areas are dominated by small aftershocks

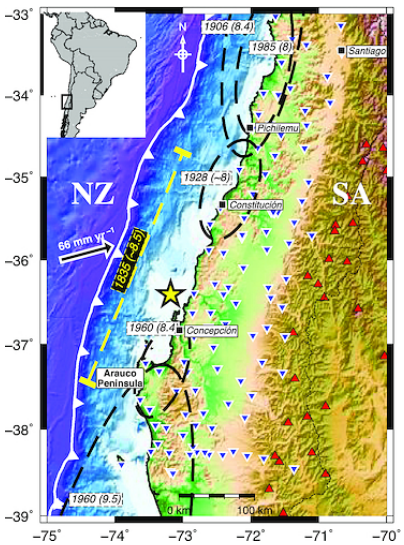

1 of 4

Experimental craters formed by single and multiple buried explosions and implications for volcanic craters with emphasis on maars

Greg A. Valentine, James D. L. White, Pierre-Simon Ross, Jamal Amin, Jacopo Taddeucci, Ingo Sonder, Peter J. Johnson

First Published: 16 October 2012 Vol: 39, L20301 | DOI: 10.1029/2012GL053716

KEY POINTS

- Craters from multiple buried explosions compared with single-explosion crater
- Diameter is a poor gauge of individual explosion energy for multi-explosion craters
- Crater shape and ejecta emplacement differ in multi- vs single-explosion

1 of 3

Space Sciences

Consequences of negative ions for Titan's plasma interaction

Stephen A. Ledvina, Stephen H. Brecht

First Published: 31 October 2012 Vol: 39, L20103 | DOI: 10.1029/2012GL053835

KEY POINTS

- Negative ions in Titan's ionosphere can effect Titan's plasma interaction
- Detectable levels of negative ions can be lost to Saturn's magnetosphere
- More work is needed to characterize the negative ions at Titan

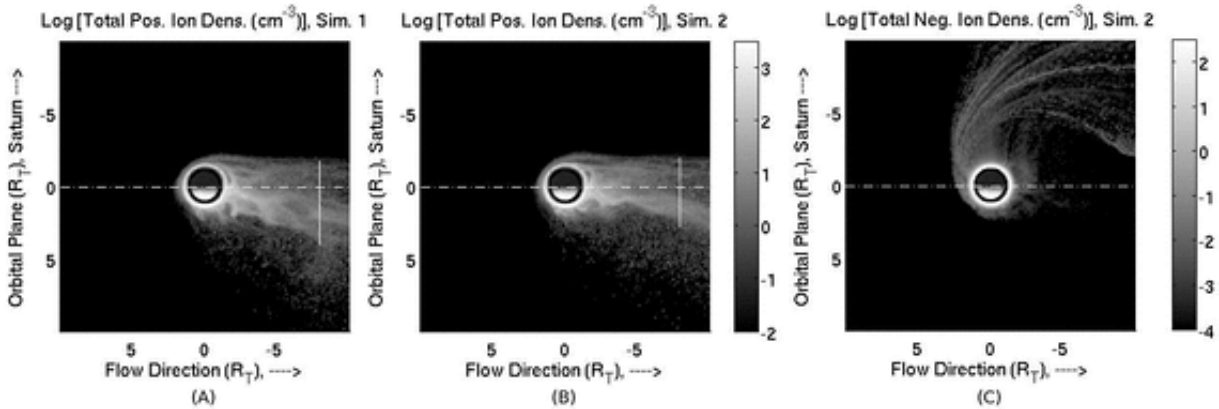

1 of 3

Enhancement of thermospheric mass density by soft electron precipitation

B. Zhang, W. Lotko, O. Brambles, M. Wiltberger, W. Wang, P. Schmitt, J. Lyon
First Published: 26 October 2012 Vol: 39, L20102 | DOI: 10.1029/2012GL053519

KEY POINTS

- Soft electron precipitation models are implemented in global simulations
- Soft electrons affect the F-region plasma state and Pedersen conductivity
- Soft electrons can cause thermospheric mass density enhancement at 400 km

Highlight

1 of 2

Monoenergetic high-energy electron precipitation in thin auroral filaments

H. Dahlgren, N. Ivchenko, B. S. Lanchester
First Published: 19 October 2012 Vol: 39, L20101 | DOI: 10.1029/2012GL053466

KEY POINTS

- Observations of monoenergetic, high energy precipitation in auroral filaments
- High resolution, multispectral observations are crucial to advance the field
- There is currently no existing consistent theory to explain the observations

1 of 3

The Cryosphere

Effects of more extreme precipitation regimes on maximum seasonal snow water equivalent

Mukesh Kumar, Rui Wang, Timothy E. Link
First Published: 31 October 2012 Vol: 39, L20504 | DOI: 10.1029/2012GL052972

KEY POINTS

- More intense snowfalls generally result in larger SWEmax
- More extreme precipitation may alleviate the decrease in SWEmax due to warming
- Sensitivity of SWEmax changes for a range of air temperature and seasonal snow

1 of 4

Recent changes in the dynamic properties of declining Arctic sea ice: A model study

Jinlun Zhang, Ron Lindsay, Axel Schweiger, Ignatius Rigor
First Published: 30 October 2012 Vol: 39, L20503 | DOI: 10.1029/2012GL053545

KEY POINTS

- Arctic sea ice volume during 2007-2011 is reduced by 33%
- Sea ice speed and deformation increase by 13% and 17%
- Ice volume export is reduced

The extreme melt across the Greenland ice sheet in 2012

S. V. Nghiem, D. K. Hall, T. L. Mote, M. Tedesco, M. R. Albert, K. Keegan, C. A. Shuman, N. E. DiGirolamo, G. Neumann

First Published: 27 October 2012 Vol: 39, L20502 | DOI: 10.1029/2012GL053611

KEY POINTS

- Satellites reveal the 2012 extreme melt across most of the Greenland ice sheet
- In-situ temperature data and field observations confirm the melt event
- Extreme melt is rare: last one in 1889, and next previous ~7 centuries earlier

Highlight

Automated mapping of Earth's annual minimum exposed snow and ice with MODIS

Thomas H. Painter, Mary J. Brodzik, Adina Racoviteanu, Richard Armstrong

First Published: 24 October 2012 Vol: 39, L20501 | DOI: 10.1029/2012GL053340

KEY POINTS

- We must systematically determine Earth's current total glacier cover
- MODICE provides annual, consistently derived map of the world's glaciers
- MODICE data support assessments of sea level rise and impacts of global warming

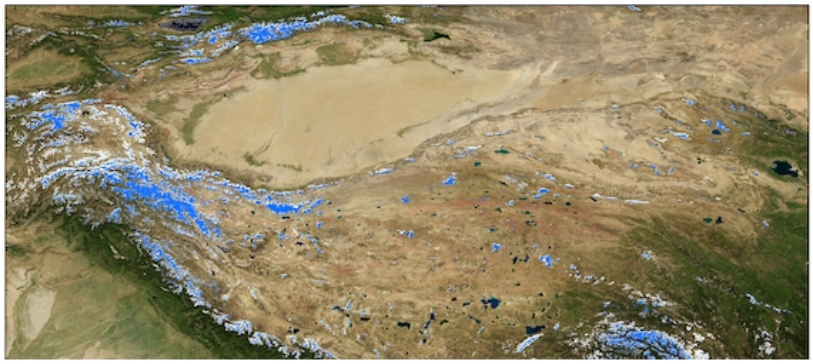

1 of 4

Current Issue

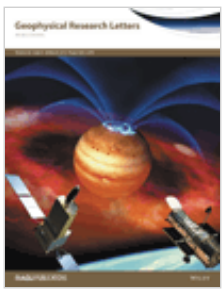

Volume 42
Issue 6
28 March 2015

All Issues
Browse a free sample issue

Find an article

volume (required) and

page or citation #

Stay Connected to Eos

Access Eos Archive Issues

Issues from 1997-2014 are freely available to the public.

Older issues are available through AGU membership or through an institutional subscription.

Journal Resources

Call for Papers
Special Section Proposal Form
Personal Choice
Terms of Use
Cover Gallery
Institutional Subscription Rates
Get RSS Feed

Featured Special Collection

The Early Results from the Van Allen Probes

NASA's Van Allen Probes mission is designed to acquire data to solve key questions about the energetics and dynamics of the Earth's Van Allen Radiation belts that have arisen from active research in the domain in the past decades.

Editors' Highlights

- What Causes Sunspot Pairs?
- Water Beneath the Surface of Mars, Bound up in Sulfates
- When Predicting Drought Risk, Do Not Overlook Temperature
- Changing Patterns in U.S. Air Quality

See all »

Download the app

Download the Geophysical Research Letters app on your iPad

Upcoming AGU Meetings

Triennial Earth-Sun Summit

26 Apr - 1 May 2015
Indianapolis, Indiana, USA

2015 Joint Assembly

3-7 May 2015
Montreal, Canada

Chapman Conference on Evolution of the Asian Monsoon and its Impact on Landscape, Environment and Society: Using the Past as the Key to the Future

14-19 June 2015
Hong Kong SAR, China

See all »

AGU PUBLICATIONS

WILEY